Int. J. Heat Mass Transfer. Vol. 12, pp. 843–848. Pergamon Press 1969. Printed in Great Britain

SIMULTANEOUS DETERMINATION OF MICROLAYER GEOMETRY AND BUBBLE GROWTH IN NUCLEATE BOILING

H. H. JAWUREK
Nuclear Engineering Division, Atomic Energy Board, Pretoria, South Africa

(*Received* 14 *June* 1968 *and in revised form* 11 *November* 1968)

Abstract—An optical technique is described which permits the simultaneous determination of detailed microlayer geometry and macroscopic bubble dynamics in nucleate boiling. Boiling takes place from a transparent heating surface forming the floor of a tank. With parallel, monochromatic illumination from below, the microlayers reflect interference patterns similar to Newton's rings. These fringe patterns are recorded by a high-speed ciné camera and provide details of microlayer shape and thickness. Simultaneously, and on the same film, normal bubble-growth pictures in profile are obtained. The optics of the system are analysed. Sample results are discussed.

NOMENCLATURE

- d, microlayer thickness [m];
- I, intensity of light waves [J/s m^2];
- m, order of interference;
- n, refractive index of glass;
- n_0, refractive index of vapour;
- n_1, refractive index of liquid;
- $\bar{x}$, path difference of light rays in microlayer ($= 2n_1 d$), [m].

Greek symbols

- κ, contrast of fringes;
- λ, wavelength of light [m];
- ρ, reflectance ($= I_{\text{reflected}}/I_{\text{incident}}$).

1. INTRODUCTION

DURING nucleate boiling thin liquid films (microlayers) form beneath and subsequently evaporate into attached bubbles [1, 2]. There is a need to establish quantitatively and for various conditions of normal boiling:

(1) the microlayer shape and thickness vs. time,
(2) the interrelation between microlayer behaviour and macroscopic bubble dynamics.

A photographic technique capable of providing this information is described.

The only previous direct measurements of microlayer thickness, those of Sharp [1], employed high-speed interference photography through the tops of bubbles flattened between the heating surface and a closely adjacent parallel window. Bubbles thus grew under abnormal conditions. Growth rate was not recorded.

In the study here described, boiling took place from a transparent, electrically heated surface forming the floor of a tank. High-speed interferometric ciné photography from below provided details of microlayer geometry. Simultaneously, and on the same film, macroscopic bubble-growth pictures in profile were recorded.

2. HEATING SURFACE

This consisted of a glass disc (Fig. 1) coated with an electrically conducting, transparent film of stannic oxide [3]. The film was in contact with the test liquid and heated by direct current. Silver current leads were attached by indium soldering [4]. A further layer of vacuum-evaporated indium accurately defined the edges of the contacts.

Discs were cut from ready-coated sheets of the commercial products "Electropane" (Libbey

Owens Ford Glass Co., U.S.A.). The stannic oxide coating had an optical thickness of half a wavelength, a refractive index of 2·0 and a resistance of 70 Ω/square. Film along the edges was removed chemically [5] to produce

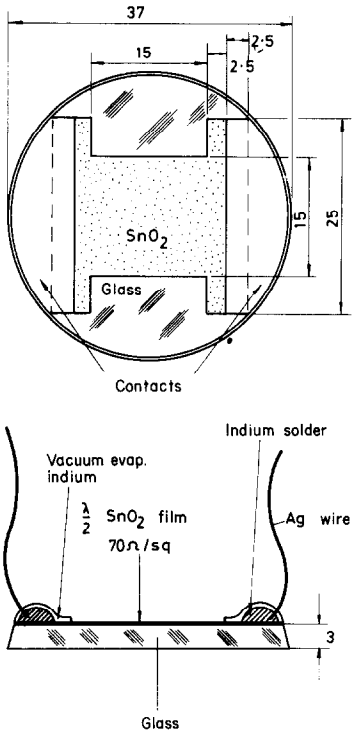

FIG. 1. Heating surface.

an H-shaped heating surface. This prevented excessive nucleation along the stannic oxide/–indium contact line.

In the middle of the disc, a small pit was scratched through the stannic oxide layer and into the glass. The pit was again rendered electrically conducting by a vacuum-evaporated indium film. The heated cavity thus produced acted as a bubble nucleation site. Under sub-atmospheric pressure large isolated bubbles and vapour columns were produced. Laterally interfering bubbles from naturally occurring nucleation sites could also be studied.

The current density over the film was determined by a conducting-sheet analogue. The gross heat flux over the central, uniformly heated section could then be calculated from measurements of the electrical input and various corrections.

The surface operated satisfactorily with many organic test liquids. Water, however, could not be boiled; both heating film and contacts were destroyed, apparently by electrolytic action.

3. BOILING TANK

The disc described formed the floor of a cylindrical boiling tank. A flat-sided water-jacket surrounding the tank provided a constant temperature bath and eliminated distortion of the bubble profile view.

Tank pressure was accurately controlled and measured.

Thermocouples measured the test liquid temperature. When desired, precise saturation temperature could be maintained by additional boiling from a heating coil suspended above the boiling disc.

4. OPTICS OF MICROLAYER INTERFEROMETRY

Consider an attached bubble with a partially evaporated microlayer as in Fig. 2. The system is illuminated from below by a normally incident, nearly parallel and nearly monochromatic beam of light. Reflections from the top and bottom of the microlayer interfere to produce localized fringes similar to Newton's rings [6].

Reflectance, ρ, of the system of two thin films (microlayer and $\lambda/2$ SnO_2 film) is evaluated and the fringe contrast calculated. For the two extreme cases of reflectance we have:

Case 1. Microlayer optical thickness is zero or an even multiple of a quarter wave, i.e.

$$n_1 d = 2m(\lambda/4), \qquad m = 0, 1, 2 \ldots \tag{1}$$

i.e. the path difference $\bar{x} = 0, \lambda, 2\lambda \ldots$.

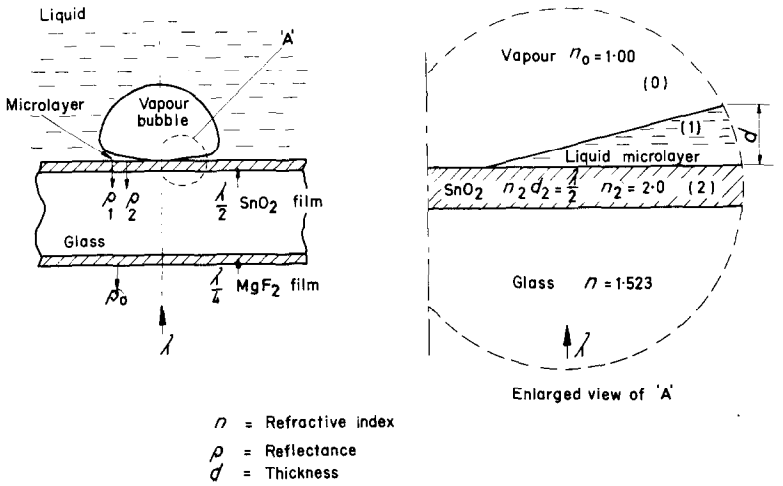

FIG. 2. Optics of microlayer interferometry.

The reflectance is then given by [7]

$$\rho_1 = [(n - n_0)/(n + n_0)]^2 \qquad (2)$$

where refractive indices, n, are defined in Fig. 2. Note that the reflectance is independent of n_1 and that n_0 can be taken as 1·00 for all vapours. Thus with a given glass the value of ρ_1 is fixed and independent of test liquid. With $n = 1{\cdot}523$ (manufacturers' value) $\rho_1 = 0{\cdot}0429$, i.e. 4·29 per cent.

Case 2. Microlayer optical thickness is an odd multiple of a quarter wave, i.e.

$$n_1 d = (2m + 1)(\lambda/4), \qquad m = 0, 1, 2 \ldots \qquad (3)$$

i.e. the path difference $\bar{x} = \lambda/2, 3\lambda/2, 5\lambda/2 \ldots$

The reflectance is then given by [7]

$$\rho_2 = [(n_1^2 - nn_0)/(n_1^2 + nn_0)]^2 \qquad (4)$$

and is now dependent on n_1 the refractive index of the test liquid.

With the contrast, κ, for the fringes defined as $(I_{\text{maxima}} - I_{\text{minima}})/I_{\text{maxima}}$, where I is light intensity, it is seen that maximum contrast ($\kappa = 1{\cdot}00$) is achieved with $\rho_2 = 0$, i.e. with $n_1 = (n)^{0{\cdot}5} = 1{\cdot}234$. No suitable liquid exists. The closest practical substitute, methanol, with $n_1 = 1{\cdot}33$, was used in most tests. Then $\rho_2 = 0{\cdot}56$ per cent and $\kappa = 0{\cdot}87$, a good contrast. The second liquid tested, ethanol, with $n_1 = 1{\cdot}36$, has $\rho_2 = 0{\cdot}93$ per cent and $\kappa = 0{\cdot}78$.

Equation (1) thus defines maxima of reflectance (light fringes), equation (3) minima (dark fringes).

Note that test liquids must be carefully chosen, since as $n_1 \to n (= 1{\cdot}523$ in our case), $\kappa \to 0$ and fringes become invisible. Alternatively, for a given test liquid a glass substrate of suitable refractive index must be found.

The reflectance ρ_0 from the bottom of the disc (see Fig. 2) is superimposed on the fringe pattern and reduces overall contrast. This effect was minimized by a magnesium fluoride anti-reflection coating [8].

5. OPTICAL SYSTEM

See Fig. 3. An interferometry beam, sufficiently parallel and monochromatic [6], was produced by a d.c.-operated mercury arc lamp, a collecting lens, a pinhole, a collimating lens and a line filter ($\lambda = 434$ nm). Front surface mirror 1 deflected the beam to impinge normally on the bottom of the boiling disc. A beam splitter directed the reflected beam towards a rotating-prism camera (16 mm Stålex).

Bubble profiles were photographed by diffuse

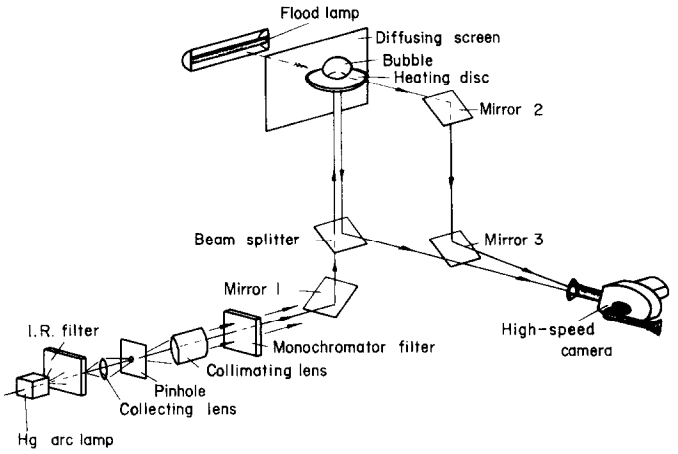

FIG. 3. Overall optical system.

transmitted light. Front-surface mirrors 2 and 3 were so arranged that the camera saw the bubble profile view and the microlayer view side by side, each occupying about half the film frame.

6. RESULTS AND DISCUSSION

Figure 4 shows portion of a typical film on isolated bubble boiling.

The two bright lines on either side of the interferogram are the indium contracts; reflection from the main body of the bubble caused the bright arc above the rings.

The light spot in the centre of the fringes represents a microlayer thickness of zero (i.e. dry patch); subsequent light rings correspond to thicknesses of $1\lambda/2\ n_1$, $2\lambda/2n_1$, $3\lambda/2n_1 \ldots$; dark rings to $1\lambda/4n_1$, $3\lambda/4n_1$, $5\lambda/4n_1 \ldots$. Microlayer thickness is thus given in steps of $\lambda/4n_1$ (= 0·082 μm for test shown).

The profile view shows the attached bubble of approximately 13 mm major diameter, current leads and thermocouples.

Analysable results were obtained for methanol and ethanol at system pressures of 20–50 kN/m^2 (approx. 0·2–0·5 atm), heat fluxes of 30–100 kW/m^2 and subcooling of 0–20°C.

In all cases microlayers were wedge-shaped in cross-section, i.e. increasing in thickness from bubble centre to edge. For fully grown bubbles, thicknesses at the outer edge ranged from 0·2 to 0·8 μm and showed no systematic trend with the parameters varied. Thickness values are lower than those estimated from indirect measurements [9, 10] and of the same order as Sharp's [1] on flattened steam bubbles.

It is generally assumed, e.g. [1, 10], that microlayers beneath growing bubbles are stagnant. Evaporation should then cause them to become progressively thinner with time. Such thinning-down (accompanied by dry-patch growth) occurred only near the inner microlayer perimeter, generally at thicknesses of less than 0·15 μm. Elsewhere local thickness increased with time. Microlayers were thus continuously replenished by liquid, with the rate of in-flow exceeding the rate of evaporative depletion.

These effects are illustrated by the sample results of Fig. 5. Test conditions are given in the figure caption. The bubble appeared after a waiting time of 262 msec and was immediately followed by several smaller bubbles of zero waiting time. This overall cycle was repeated throughout the test run. (Similar boiling occurred during the tests of Figs. 4 and 8.)

Figure 5(a) shows the development of the bubble profile.

Figure 5(b) gives a detailed microlayer history. The bubble base radii, r, at which microlayer

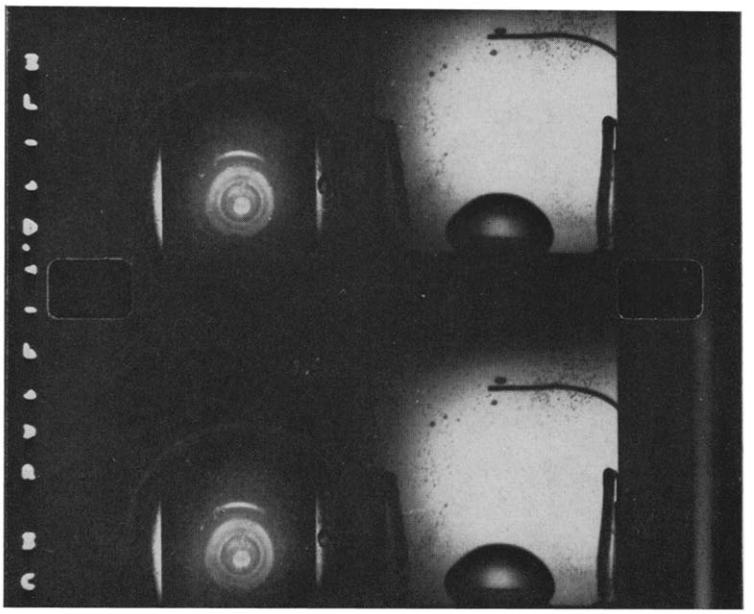

FIG. 4. *Isolated bubble boiling;* microlayer interferogram on left, bubble profile view on right. Test liquid methanol; gross heat flux 70 kW/m², pressure 25·6 kN/m², subcooling 10·4°C. Interval between frames 1·00 msec.

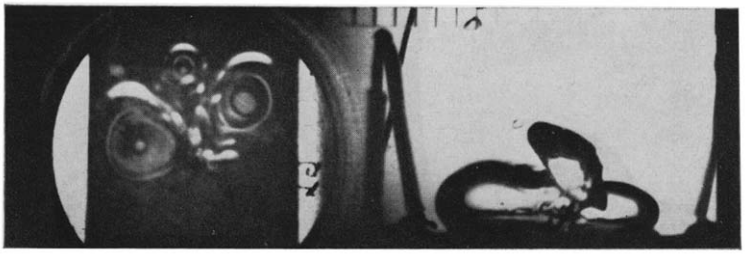

FIG. 6. *Laterally interacting bubbles* with microlayers distorted but intact. Test liquid ethanol; gross heat flux 65·9 kW/m², pressure 25·4 kN/m², subcooling 2·6°C.

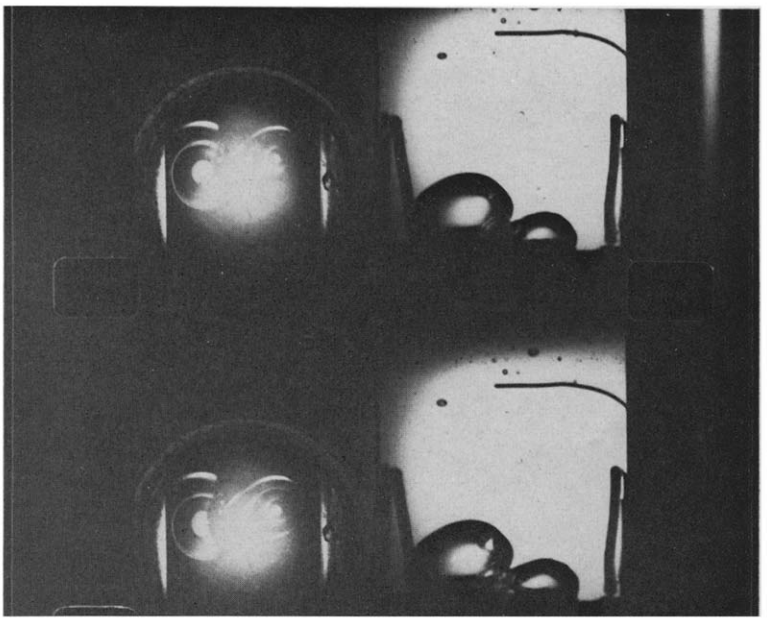

FIG. 7. *Laterally interacting bubbles* with left-hand microlayer and dry patch being flooded. Test liquid methanol, gross heat flux 87·1 kW/m^2 pressure 25·6 kN/m^2, subcooling 7·9°C. Interval between frames 2·15 msec.

FIG. 8. *Bubble with zero waiting time and irregular microlayer.* Test liquid ethanol; gross heat flux 69·8 kW/m^2, pressure 25·4 kN/m^2 subcooling 4·8°C.

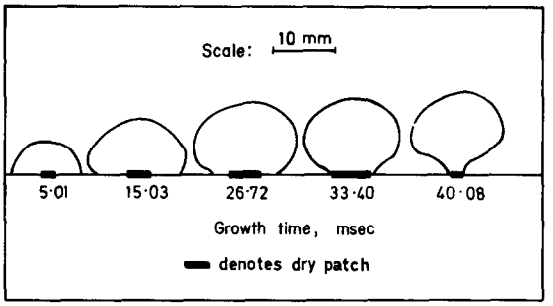

FIG. 5(a). Bubble profiles for Run M13. Test liquid methanol, gross heat flux 62·3 kW/m², pressure 24·0 kN/m², subcooling 7·1°C.

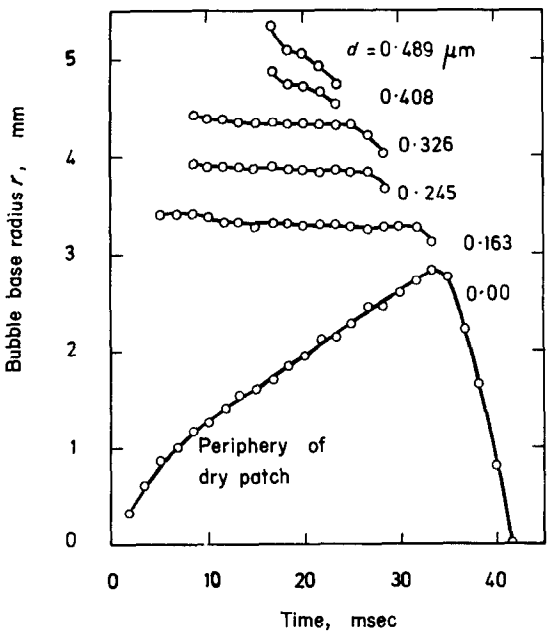

FIG. 5(b). Detailed microlayer history, Run M13.

thicknesses, d, of 0, $2\lambda/4n_1$, $3\lambda/4n_1$, $4\lambda/4n_1$... occur are plotted against time. (The position of the first minimum, $d = 1\lambda/4n_1$, could not be determined with accuracy.) The positive slope of the curve for $d = 0$ illustrates microlayer thinning and dry patch growth. For $d \geqslant 2/4n_1$ ($= 0{\cdot}163$ μm) the slopes are negative, i.e. microlayer thickness is increasing. Figure 5(c), a replot for selected time steps, shows this effect more clearly.

Special numerical methods for the estimation of the evaporation rate under such conditions of in-flow are needed. From these, and from the bubble growth records, it will be possible to determine the contribution of microlayer evaporation to total bubble growth.

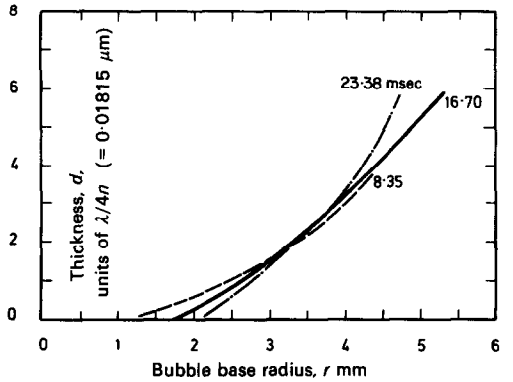

FIG. 5(c). Microlayer profiles, Run M13.

Figures 6 and 7 show boiling that might well occur in practical systems. Bubbles from naturally occurring nucleation sites interfere laterally. Figure 6 illustrates weak microlayer interaction. Figure 7 shows strong interaction: the right hand bubble caused destruction of the microlayer and dry patch of its neighbour and forced it into premature detachment.

Microlayers of bubbles with zero waiting time suffered disturbances ranging from mild fringe distortion to total fragmentation. Figure 8 illustrates an intermediate case.

These sample results seem to indicate that the technique described is a powerful tool in microlayer studies.

It should be remembered that the photographs in Figs. 4, 6, 7 and 8 are reproductions of prints and do not show the detail available to the author.

ACKNOWLEDGEMENTS

This work was started in the Mechanical Engineering Department, University of the Witwatersrand and executed mainly in the Nuclear Engineering Division of the Atomic Energy Board. The author is deeply grateful to these institutions, their Heads and Staff.

Warmest thanks are offered to Mr. D. J. Maritz for experimental assistance and to Drs. C. J. Rallis and I. E. Bock for guidance and discussions.

REFERENCES

1. R. R. SHARP, The nature of liquid film evaporation during nucleate boiling. *NASA TN D*-1997, Lewis Research Centre, Cleveland, Ohio (1964).
2. K. TORIKAI and T. YAMAZAKI, The contact area of boiling bubbles on the heating surface, *Bull. Jap. Soc. mech. Engrs* **8**, 660–669 (1956).
3. R. E. AITCHISON, Transparent semi-conducting oxide films, *Aust. J. Appl. Sci.* **5**, 10–17 (1954).
4. R. B. BELSER, A technique of soldering to thin metal films, *Rev. Sci. Instrum.* **22**, 180 (1954).
5. M. S. TARNOPOL, Treatment of films with liquid, *U.S. Pat.* 2606566 (1952).
6. M. FRANÇON, *Optical Interferometry*. Chap. 3. Academic Press, New York (1966).
7. A. VAŠÍČEK, *Optics of Thin Films*, p. 176. North-Holland, Amsterdam (1960).
8. L. HOLLAND, *Vacuum Deposition of Thin Films*, pp. 270–281. Chapman & Hall, London (1958).
9. N. B. HOSPETI and R. B. MESLER, Deposits formed beneath bubbles during nucleate boiling of radioactive calcium sulfate solutions, *Chem. Engng Progr. Symp. Ser.* **62**, 72–76 (1966).
10. M. G. COOPER and A. J. P. LLOYD, Transient local heat flux in nucleate boiling, *Proc. 3rd Int. Heat Transf. Conf.* **3**, 193–203, Chicago (1966).

Résumé—On décrit une technique optique qui permet la détermination simultanée de la géométrie détaillée de la microcouche et de la dynamique macroscopique détaillée des bulles dans l'ébullition nucléée. L'ébullition a lieu à partir d'une surface transparente formant le plancher d'un réservoir. Les microcouches produisent, en éclairant par en-dessous avec de la lumière monochromatique, à rayons parallèles, des figures d'interférences semblables à des anneaux de Newton. Ces ensembles de franges sont enregistrés par une caméra à grande vitesse et fournissent des détails sur la forme et l'épaisseur de la microcouche. On obtient simultanément sur le même film les profils de croissance normale des bulles. On analyse l'optique du système et l'on discute quelques résultats.

Zusammenfassung—Es wird eine optische Technik beschrieben, die es erlaubt, die Geometrie der Mikrogrenzschicht im Einzelnen festzustellen und gleichzeitig die Blasendynamik zu untersuchen. Das Sieden findet auf einer transparenten Oberfläche statt, die den Boden eines Behälters bildet. Bei paralleler monochromatischer Beleuchtung von unten reflektiert die Mikrogrenzschicht Interferenzfiguren ähnlich den Newton'schen Ringen. Diese Streifenmuster wurden mit einer Hochgeschwindigkeitsfilmkamera aufgenommen und geben Einzelheiten der Gestalt und Dicke der Mikrogrenzschicht wieder. Zugleich und Dicke der Mikrogrenzschicht wieder. Zugleich und auf demselben Film ist die Blasenbildung in Profilaufnahmen festgehalten. Das verwendete optische Verfahren wurde analysiert und die Ergebnisse diskutiert.

Аннотация—Описан оптический метод, который позволяет одновременно подробно изучать конфигурацию микрослоя и динамику макроскопических пузырьков при пузырьковом кипении. Кипение просходит на прозрачной поверхности, образующей основание бака. При параллельном монохроматическом освещении снизу микрослои дают интерференционные картинки аналогичные ньютоновским кольцам. Эти картинки регистрировались высокоскоростной кинокамерой и позволяют наблюдать изменения в конфигурации микрослоя и его толщины. На этой же пленке одновременно регистрировались обычные картины роста пузырьков в профиль. Анализируется оптика системы. Обсуждаются результаты образцов картинок.